Cancer Cell
Article

# Double Antiangiogenic Protein, DAAP, Targeting VEGF-A and Angiopoietins in Tumor Angiogenesis, Metastasis, and Vascular Leakage

Young Jun Koh,[1,2,9] Hak-Zoo Kim,[1,2,9] Seong-Ik Hwang,[1,3] Jeung Eun Lee,[1,3] Nuri Oh,[1,3] Keehoon Jung,[1,2] Minah Kim,[1,3] Kyung Eun Kim,[1,2] Homin Kim,[3] Nam-Kyu Lim,[5] Choon-Ju Jeon,[5] Gyun Min Lee,[3,4] Byeong Hwa Jeon,[6] Do-Hyun Nam,[7] Hoon Ki Sung,[8] Andras Nagy,[8] Ook Joon Yoo,[2] and Gou Young Koh[1,2,3,4,7,*]
[1]National Research Laboratory of Vascular Biology and Stem Cells
[2]Graduate School of Biomedical Science and Engineering
[3]Department of Biological Sciences
[4]Graduate School of Nanoscience and Technology
Korea Advanced Institute of Science and Technology (KAIST), Daejeon, 305-701, Korea
[5]Aprogen Inc., Daejeon, 305-701, Korea
[6]Department of Physiology, School of Medicine, Chungnam National University, Daejeon, 301-131, Korea
[7]Institute for Refractory Cancer Research Program, Samsung Medical Center, Sungkyunkwan University School of Medicine, Seoul, 135-710, Korea
[8]Department of Molecular Genetics, University of Toronto, Samuel Lunenfeld Research Institute, Mount Sinai Hospital, Ontario M5G 1X5, Canada
[9]These authors contributed equally to this study
*Correspondence: gykoh@kaist.ac.kr
DOI 10.1016/j.ccr.2010.07.001

## SUMMARY

**Two vascular growth factor families, VEGF and the angiopoietins, play critical and coordinate roles in tumor progression and metastasis. A single inhibitor targeting both VEGF and angiopoietins is not available. Here, we developed a chimeric decoy receptor, namely double anti-angiogenic protein (DAAP), which can simultaneously bind VEGF-A and angiopoietins, blocking their actions. Compared to VEGF-Trap or Tie2-Fc, which block either VEGF-A or angiopoietins alone, we believe DAAP is a highly effective molecule for regressing tumor angiogenesis and metastasis in implanted and spontaneous solid tumors; it can also effectively reduce ascites formation and vascular leakage in an ovarian carcinoma model. Thus, simultaneous blockade of VEGF-A and angiopoietins with DAAP is an effective therapeutic strategy for blocking tumor angiogenesis, metastasis, and vascular leakage.**

## INTRODUCTION

The orchestrated actions of multiple growth factors and their receptors, coreceptors, and binding partners are required for tumor angiogenesis (Ferrara and Kerbel, 2005; Folkman, 2007). Of these factors, VEGF-A is a prime molecule responsible for tumor progression and metastasis by enhancing angiogenesis and vascular leakage (Ferrara and Kerbel, 2005; Folkman, 2007). Several approaches have been developed to block VEGF-A action, including blocking antibody, decoy receptor, and siRNA against VEGF-A, and clinical applications are currently being tested (Ferrara et al., 2004; Holash et al., 2002; Hurwitz et al., 2004) (Angiogenesis Inhibitors in Clinical Trials, National Cancer Institute, http://www.cancer.gov/clinicaltrials/developments/anti-angio-table/). When developing therapeutic decoy receptor proteins, the binding affinity, efficacy, half-life, bioavailability, molecular size, stability, and effectiveness should be considered (Holash et al., 2002; Shibuya and Claesson-Welsh, 2006). To fulfill

### Significance

The effective blockade of tumor angiogenesis and vascular leakage with more than a single targeting molecule has been shown to be effective in preventing tumor growth and metastasis. By developing a double decoy receptor, DAAP, which can simultaneously bind VEGF-A and angiopoietins, this study demonstrated that the double blockade of VEGF-A and angiopoietins is highly effective for reducing tumor angiogenesis, metastasis, and vascular leakage, with greater effects over the single blockade of VEGF-A or angiopoietins. This proof-of-concept using DAAP introduces a strategic approach to effectively controlling tumor growth and metastasis, and the generation of DAAP provides a "double trap" using a single molecule, thus presenting a therapeutic protein.

these considerations, Holash et al. (2002) developed an elegant therapeutic VEGF-A decoy receptor protein, VEGF-Trap. VEGF-Trap is a chimeric protein consisting of the second immunoglobulin-like (Ig-like) domain (Ig2) of VEGFR1, the third Ig-like domain (Ig3) of VEGFR2, and the Fc portion of human IgG (Fc). VEGF-Trap exhibits picomolar binding affinity to VEGF-A and displays high bioavailability in vivo with low extracellular matrix (ECM) binding and a moderate half-life (Holash et al., 2002). Several studies (Byrne et al., 2003; Holash et al., 2002; Saishin et al., 2003; Verheul et al., 2007) indicate that VEGF-Trap not only effectively inhibits tumor- and ocular-angiogenesis, but also substantially reduces vascular leakage, which arises from the actions of VEGF-A and its receptors, mainly VEGFR2 and, to a lesser extent, VEGFR1 in vivo. VEGF-Trap fulfills the most critical points for developing therapeutic decoy receptor proteins that block VEGF-A in vivo. However, VEGF-Trap blocks only VEGF-A and placental growth factor (PlGF) among multiple endothelial growth factors involved in tumor angiogenesis.

Angiopoietins, in concert with VEGF-A, are another family of growth factors that modulate tumor angiogenesis mediated through Tie2 receptor, which is highly expressed in growing blood endothelial cells (Augustin et al., 2009; Holash et al., 1999; Shim et al., 2007; Yoshiji et al., 2005). Angiopoietins include four proteins: Ang-1, Ang-2, Ang-3, and Ang-4. Among them, Ang-2 alone regresses blood vessels, whereas Ang-2 expression precedes VEGF-A expression in growing tumor vessels and enhances angiogenesis in the presence of VEGF-A (Holash et al., 1999). Indeed, accumulating evidence (Augustin et al., 2009; Huang et al., 2009; Shim et al., 2007) indicates that Ang-2 in concert with VEGF-A act as promoting molecules for tumor angiogenesis and metastasis. Accordingly, a specific blocking antibody or peptibody against Ang-2 reduces tumor angiogenesis, and growth in some tumor models (Brown et al., 2010; Hashizume et al., 2010; Oliner et al., 2004). In contrast, Ang-1 acts as an inhibiting molecule for tumor growth by inhibiting leakage and enhancing stabilization of tumor vessels (Ahmad et al., 2001). Moreover, a recent report indicates that endogenous Ang-1 could lead to normalization of tumor vessels during selective blockade of Ang-2 action (Falcon et al., 2009). However, several reports indicate that the upregulation of Ang-1 and Ang-2 is part of "angiogenic rescue" when VEGF-A-VEGFR2 signaling is blockaded during tumor progression, exaggerating malignant tumor progression by increasing local invasion and accelerating metastasis (Casanovas et al., 2005; Ebos et al., 2009; Huang et al., 2009; Paez-Ribes et al., 2009). Therefore, we envisioned that a double blockade of VEGF-A and angiopoietins could effectively inhibit tumor angiogenesis and metastasis.

Here, we describe a chimeric protein molecule, double antiangiogenic protein (DAAP), as a dual decoy receptor for VEGF-A/PlGF and angiopoietins.

## RESULTS

### Generation of DAAP

To design a double decoy receptor for VEGF-A and angiopoietin, we used the Ig2 of VEGFR1 or Ig2 and Ig3 of VEGFR1 as a VEGF-A decoy molecule and the minimal binding domain of ECD-Tie2 as an angiopoietin decoy molecule (Figure 1A). To identify a minimal but effective binding domain of the Tie2 receptor for Ang-2, a series of ECD-Tie2 deletion mutations and ELISA binding assays were used (Figure S1A available online). In ECD-Tie2, Ig2 is essential for angiopoietin binding, but Ig1 and three EGF-like domains (E123) seem to be required for stable angiopoietin binding. The Ig1-Ig2-E123 of Tie2 (amino acids 1–348) was the effective and minimal size of the Ang-2 binding protein, and its Ang-2 binding activity was similar to ECD-Tie2, in agreement with previous reports (Macdonald et al., 2006). Importantly, the Ig1-Ig2-E123 of Tie2 contains 11.7% acidic amino acids and has a theoretical pI of 6.55. Based on these findings, seven different combinations of DAAP were made with different combinations of (Ig2 or Ig2-Ig3 of VEGFR1), (Ig2, Ig1-Ig2, or Ig1-Ig2-E123 of Tie2) and the Fc portion of the IgG antibody, named DAAP1-7 (Figure 1B). ELISA analyses revealed that DAAP-1, -2, -3, -6, and -7 were incapable of binding to both VEGF-A and Ang-2, whereas DAAP-4 and DAAP-5 were capable of binding both VEGF-A and Ang-2, indicating that the proper alignment of the Ig-like domains is required for appropriate binding to the ligand. We chose DAAP-5, hereafter referred to as DAAP, as the best candidate because deletion of VEGFR1 Ig3 from DAAP-4 did not significantly alter its binding character, which is consistent with previous findings (Davis-Smyth et al., 1996), and the molecular size of DAAP-5 was less than that of DAAP-4. Further analyses were done with VEGF-Trap and Tie2-Fc.

### Characterization of DAAP

In vitro pull-down assays revealed that DAAP is able to bind to human (h) VEGF-$A_{165}$, mouse (m) VEGF-$A_{164}$, hVEGF-$A_{189}$, hVEGF-$A_{121}$, mPlGF, hAng-2, mAng-2, hAng-1, mAng-3, and hAng-4, but it is not able to bind to hVEGF-C, VEGF-E, human angiopoietin-like-2 (hAngptl-2), or mAngptl-4 (Figure 1C). Consistent with previous data (Holash et al., 2002), VEGF-Trap was able to bind all VEGF-A isoforms tested but not any of the angiopoietins, whereas Tie2-Fc was able to bind all angiopoietins tested but not any VEGF (Figures 1D and 1E). These data indicate that DAAP is capable of binding VEGF-A isoforms, PlGF, and angiopoietin family proteins. Accordingly, DAAP almost completely inhibited VEGF-A- or Ang-1-induced VEGFR2 or Tie2 activation in primary cultured endothelial cells (Figures S1B and S1C). Both DAAP and VEGF-Trap potently blocked VEGF-A (2.5 nM)-induced proliferation in primary cultured endothelial cells, with the $IC_{50}$ (the concentration that results in half-maximal inhibition) at 0.98 ± 0.08 nM (n = 4) and 1.06 ± 0.13 nM (n = 4), respectively. ELISA analyses revealed that the binding affinity of DAAP to VEGF-A is roughly three times lower than that of VEGF-Trap to VEGF-A, whereas the binding affinity of DAAP to Ang-2 is roughly five times higher than that of Tie2-Fc to Ang-2 (Figures 1D and 1E). BIAcore analyses showed similar results (Figure S1D). DAAP is a disulfide-linked dimer of approximately 170 kDa (Figure S1E). Five N-glycosylation and no O-glycosylation sites were predicted in DAAP (Figure S1F). A deglycosylation assay with several glycosidases indicated that DAAP is an N-glycosylated protein with terminal sialic acids, but it is not an O-glycosylated protein (Figure S1G). The N-glycosylation of DAAP does not seem to be important for its VEGF-A or Ang-2 binding activities. However, it is essential for the shift of the theoretical pI value (7.7) to an observed pI value of 6.0 (data not shown). Our ELISA assays indicated that the preoccupation of one binding site on DAAP

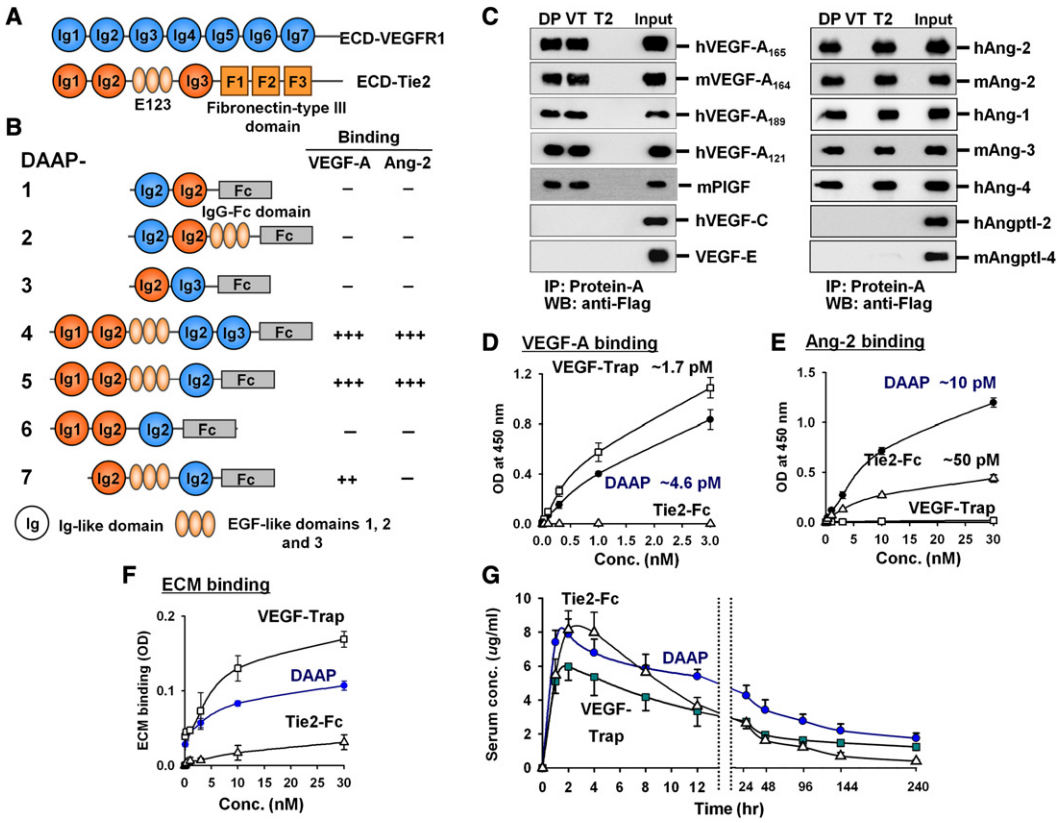


**Figure 1. Molecular and Biochemical Characteristics and Pharmacokinetic Profiles of DAAP**

(A) Schematic diagrams outlining the protein structure of the extracellular domains (ECD) of VEGFR1 and Tie2.

(B) The binding of seven DAAP variants to VEGF-A and Ang-2, was determined by ELISA and graded by binding affinity: none (–), weak (+), moderate (++), and strong (+++).

(C) In vitro binding assay between DAAP (DP), VEGF-Trap (VT), or Tie2-Fc (T2) and various VEGF isoforms, PlGF, angiopoietins, or Angptls. h, human; m, mouse. The immunoprecipitates were captured by Protein-A and western blotted with anti-FLAG antibody. Input, input of each recombinant protein loaded for comparison.

(D–F) Comparison of bindings of DAAP, VEGF-Trap, and Tie2-Fc to (B) VEGF-A, (C) Ang-2, or (D) ECM as determined by ELISA. Numbers in (B) and (C) indicate the binding affinity. Values are mean ± SD (n = 4).

(G) Pharmacokinetic profiles for DAAP. DAAP, VEGF-Trap, or Tie2-Fc (100 μg) was subcutaneously injected into C57BL/6J mice, blood samples were taken at the indicated time points, and the serum levels of these proteins were measured by ELISA. Values are mean ± SD (n = 4).

See also Figure S1 and Table S1.

with VEGF-A or Ang-2 further enhanced its binding activity to the other ligand- Ang-2 or VEGF-A (Figures S1I–S1L), possibly through a favorable conformational change, which could be a supplementary benefit.

## DAAP Pharmacokinetics

The theoretical pI of DAAP is 7.7, but isoelectric gel focusing analysis showed its virtual pI value to be roughly 6.0 (Figure S1H). In general, therapeutic proteins with higher (>9.0) pI values display poor pharmacokinetic properties due to the highly positively charged protein being largely deposited at the site of subcutaneous injection because of the nonspecific adhesion of highly negatively charged proteoglycans that comprise the ECM. To confirm this prediction, an ECM binding assay was performed with increasing concentrations of DAAP, VEGF-Trap, and Tie2-Fc (Figure 1F). Correlating with the theoretical pI values, the ECM binding of Tie2-Fc was relatively low. The ECM binding of DAAP was higher than that of Tie2-Fc but lower than that of VEGF-Trap in the range of 3–30 nM ECM. In a standard pharmacokinetic analysis, mice were given single subcutaneous injections of 100 μg DAAP, VEGF-Trap, or Tie2-Fc recombinant protein. The half life of DAAP was longer than Tie2-Fc and VEGF-Trap (Figure 1G). DAAP had a maximal concentration ($C_{max}$) of 7.89 ± 0.96 μg/ml and a total area under the curve concentration (AUC) of 19.6 ± 2.4 μg days/ml, VEGF-Trap had a $C_{max}$ of 5.97 ± 0.60 μg/ml and an AUC of 11.9 ± 0.73 μg days/ml, and Tie2-Fc had a $C_{max}$ of 8.16 ± 0.92 μg/ml and an AUC of 10.3 ± 1.02 μg days/ml. Thus, the pharmacokinetic profiles followed the theoretical charge predictions and in vitro ECM adhesion properties, and DAAP had a higher bioavailability and longer half-life than VEGF-Trap.

## Potential Toxicity of DAAP

We examined the potential toxicity of DAAP (25 mg/kg of body weight, subcutaneous administration every 3 days for 30 days) by measuring changes in body weight, hematopoietic profile, renal function, hepatic function, and blood pressure and by morphological analyses of major organs and blood vessels

compared to other treatments, such as PBS, Fc, VEGF-Trap, and Tie2-Fc. Overall, no obvious or significant differences were found except thrombocytosis, hypertension and microalbuminuria in response to DAAP and VEGF-Trap compared to PBS, Fc, and Tie2-Fc (Table S1 and Figures S1M–S1R). Furthermore, we examined the immune response against DAAP using serum derived from mice treated with DAAP (25 mg/kg of body weight, subcutaneous administration every 3 days for 60 days). However, no notable immune responses against the junction peptide or the targeting receptors were detected using the serum (Figures S1S–S1U).

## DAAP Suppresses Tumor Growth in the LLC Implantation Tumor Model

To explore the value of DAAP as an anti-angiogenic therapeutic molecule and compare it to other effective agents targeting the VEGF-A or angiopoietins pathway, we evaluated the ability of DAAP to block tumor growth and angiogenesis in the subcutaneously implanted Lewis lung carcinoma (LLC) tumor model. After implanting $1 \times 10^6$ LLC cells, the mice were left for 7 days, allowing a small nodule (200 $mm^3$) to grow. The mice received subcutaneous injections of 5, 10, 25, and 50 mg/kg of DAAP, VEGF-Trap, Tie2-Fc, or Fc (as a control) every 3 days for the subsequent 3 weeks, and the tumor growth was measured every 6 days. Compared to Fc and Tie2-Fc treatment, tumor growth was markedly attenuated with DAAP and VEGF-Trap treatment (Figure S2A). Distinct dose-responses were observed among 5, 10, and 25 mg/kg DAAP- and VEGF-Trap-treated animals in the reduction of tumor growth, whereas no distinct differences were observed between 25 and 50 mg/kg DAAP- and VEGF-Trap-treated groups (Figure S2A). In comparison, a distinct dose-response curve for tumor growth reduction was not observed with Tie2-Fc treatment (Figure S2A). Because 25 mg/kg DAAP and VEGF-Trap administration exerted maximal effect in reducing tumor growth, we chose this dosage for subsequent experiments. Compared to Fc treatment, the increase in tumor volume was reduced 81% by DAAP and 68% by VEGF-Trap 24 days after treatment (Figure 2A). Nonetheless, compared to Fc treatment, the ratio of viable versus necrotic areas in tumors was similarly reduced by DAAP (51%) and by VEGF-Trap (52%) 24 days after treatment (Figures S2B–D). Day 31 after tumor implantation, the mice were killed, and the blood vessels in the tumors and metastatic tumor cells in the inguinal lymph nodes (LN) were evaluated. In comparison with Fc treatment, blood vessel densities were ~82% less by DAAP and 58%–60% less by VEGF-Trap in both intratumoral and peritumoral regions (Figures 2B and 2C). Importantly, detailed microscopic analysis revealed that ~70%–80% of the blood vessels in the tumors were pruned with VEGF-Trap treatment, narrowed with Tie2-Fc treatment, and pruned and narrowed with DAAP treatment regardless of the tumor region, with the exception of necrotic regions (Figure 2B). These findings indicate that DAAP not only regresses VEGF-A-induced active vessel sprouting and network formation, but also blocks angiopoietins-induced active vessel enlargement in tumor angiogenesis (Augustin et al., 2009). Accordingly, more tumor hypoxia was induced by DAAP than by VEGF-Trap (Figures S2E and S2F), confirming that DAAP is more effective than VEGF-Trap at inducing tumor vessel regression and reducing subsequent blood flow in the established tumor. Nevertheless, enhanced invasiveness of the LLC tumor was not detected at 5 and 10 days after starting treatment with DAAP and VEGF-Trap (Figure S2G). Instead, at least in the LLC implantation model, both DAAP and VEGF-Trap suppressed invasion into the surrounding skin and muscle layers (Figure S2G). We further examined the effect of DAAP and VEGF-Trap in the established LLC tumor (tumor size at start of treatment was roughly 500 $mm^3$; Figures S2H and S2I). Even under these circumstances, 60%–70% of blood vessels in the tumors were pruned with VEGF-Trap treatment but pruned and narrowed with DAAP treatment (Figure S2I). Accordingly, the effect of DAAP on antitumor growth in the established LLC tumor was significantly greater than that of VEGF-Trap (Figures S2H). To examine the effect of recombinant proteins on LLC metastasis into the sentinel LN, we sampled the inguinal LN 24 days after treatment. Treatment with DAAP, VEGF-Trap, or Tie2-Fc reduced metastasis in the order DAAP > VEGF-Trap > Tie2-Fc > Fc (Figures 2D and 2E).

## DAAP Reduces Tumor Growth and Metastasis in a Melanoma Implantation Model

We generated a melanoma model by implanting $1 \times 10^6$ B16/F10 melanoma cells into the flank region of C57BL/6J mice. Seven days later, the mice received subcutaneous injections of 25 mg/kg Fc, DAAP, or VEGF-Trap every 2 days for the subsequent 2 weeks and the tumors were sampled. Compared to Fc treatment, the increases in tumor volume were reduced 57% by DAAP and 28% by VEGF-Trap 2 weeks after treatment (Figure 3A). In comparison with Fc treatment, blood vessel densities in the intratumoral and peritumoral regions were 82% and 67% less by DAAP and 71% and 46% less by VEGF-Trap (Figures 3B and 3C). Moreover, in comparison with Fc treatment, lymphatic vessel density in the peritumoral region was 73% less by DAAP and 43% less by VEGF-Trap (Figures 3B and 3D). Compared to Fc treatment, metastasized cytokeratin$^+$ tumor cells in the inguinal and axillary LN were 94% and 88% less by DAAP and 62% and 75% less by VEGF-Trap (Figures 3E and 3F). Moreover, the number of tumor colonies (>200 μm in diameter per section) in the lungs was 93% less by DAAP and 55% less by VEGF-Trap (Figures 3G and 3H).

## Combined Therapy with DAAP Plus Cytotoxic Agent Exerts Markedly Greater Effects Than DAAP Alone

We performed additional experiments to assess the efficacy of combination therapy with DAAP and a representative cytotoxic chemotherapy agent compared to DAAP alone. Starting from 7 days after implanting $1 \times 10^6$ LLC cells or B16/F10 cells, the mice were treated with combined subcutaneous injections of 10 mg/kg DAAP or VEGF-Trap and intraperitoneal injections of 10 mg/kg cisplatin or 20 mg/kg dacarbazine (Figure 4 and Figure S3). Control mice were treated with 10 mg/kg Fc or each therapeutic individually in the same manner. In all cases, combined therapy resulted in markedly greater effects than monotherapy in reducing tumor growth, angiogenesis, and metastasis to inguinal LN and lung (Figure 4 and Figure S3). Roughly, combinations of 10 mg/kg DAAP with 10 mg/kg cisplatin or with 20 mg/kg dacarbazine resulted in antitumor growth, anti-angiogenic, and anti-metastatic effects similar to 25 mg/kg DAAP alone in both tumor models. Thus, by using

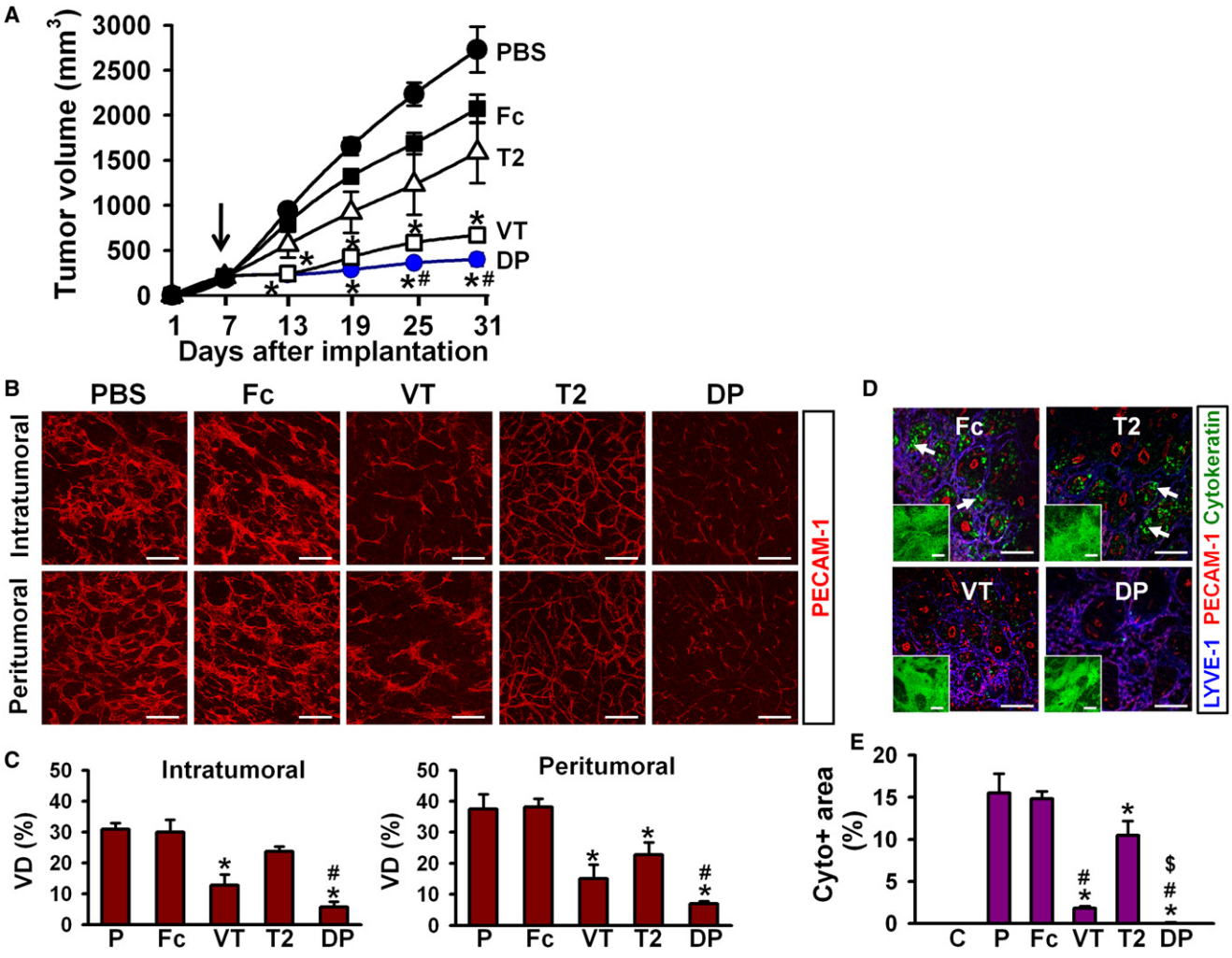


**Figure 2. DAAP Reduces Tumor Growth, Vessel Formation, and Metastasis in Implanted LLC Tumors**

(A) Comparison of tumor growths. Each group, n = 6. *$p < 0.05$ versus Fc; #$p < 0.05$ versus VT. The arrow indicates the start of injections.

(B) Images showing PECAM-1$^+$ blood vessels (red) in the peri- and intratumoral regions. Scale bars represent 200 μm.

(C) Densities of PECAM-1$^+$ blood vessels in the peri- and intratumoral regions. Each group, n = 6. *$p < 0.05$ versus Fc; #$p < 0.05$ versus VT.

(D) Images showing the presence of cytokeratin$^+$ LLC cells (green) in the inguinal LN (white arrows) and primary tumors (inlets). Scale bars represent 100 μm and 200 μm (inlets).

(E) Comparison of the metastasis of cytokeratin$^+$ LLC cells in the inguinal LN. The area of cytokeratin$^+$ fluorescence was presented as % per total sectioned area [Cyto$^+$ area (%)]. Each group, n = 6. *$p < 0.05$ versus Fc; #$p < 0.05$ versus T2; $$p < 0.05$ versus VT. All following values are mean ± SD. DP, DAAP; VT, VEGF-Trap; Fc, dimeric-Fc (Fc).

See also Figure S2.

combination therapy, the dosage of DAAP for treating cancer can be reduced by 60% and results in a similar extent of tumor growth suppression and metastasis inhibition. Equally, the possible side effects of DAAP and cisplatin or dacarbazine can be reduced by combination therapy.

## DAAP Is Superior to Combined Therapy of VEGF-Trap Plus Tie2-Fc

To compare the antitumor effect of DAAP with the antitumor effect of combination treatment with VEGF-Trap and Tie2-Fc, we determined the dosages for treatment based on molar mass and similar numbers of each protein binding to VEGF-A and angiopoietins. Given the estimations, the mice were treated with 14 mg/kg DAAP or 12 mg/kg VEGF-Trap plus 22 mg/kg Tie2-Fc every 3 or 2 days for 2 weeks, starting from 7 days after implanting $1 \times 10^6$ LLC cells or $1 \times 10^6$ B16/F10 cells (Figure 5 and Figure S4). Control mice were treated with 12 mg/kg Fc in the same manner. Compared to VEGF-Trap plus Tie2-Fc, DAAP had greater antitumor growth, anti-angiogenic, and anti-metastatic effects in both tumor models (Figure 5 and Figure S4).

## DAAP Also Reduces Tumor Growth and Metastasis in Orthotopically Implanted CT-26-luc Colon Cancer and Spontaneous Breast Tumor Models

To determine whether DAAP is more uniformly efficacious than VEGF-Trap in antitumor effect, we compared the efficacy of

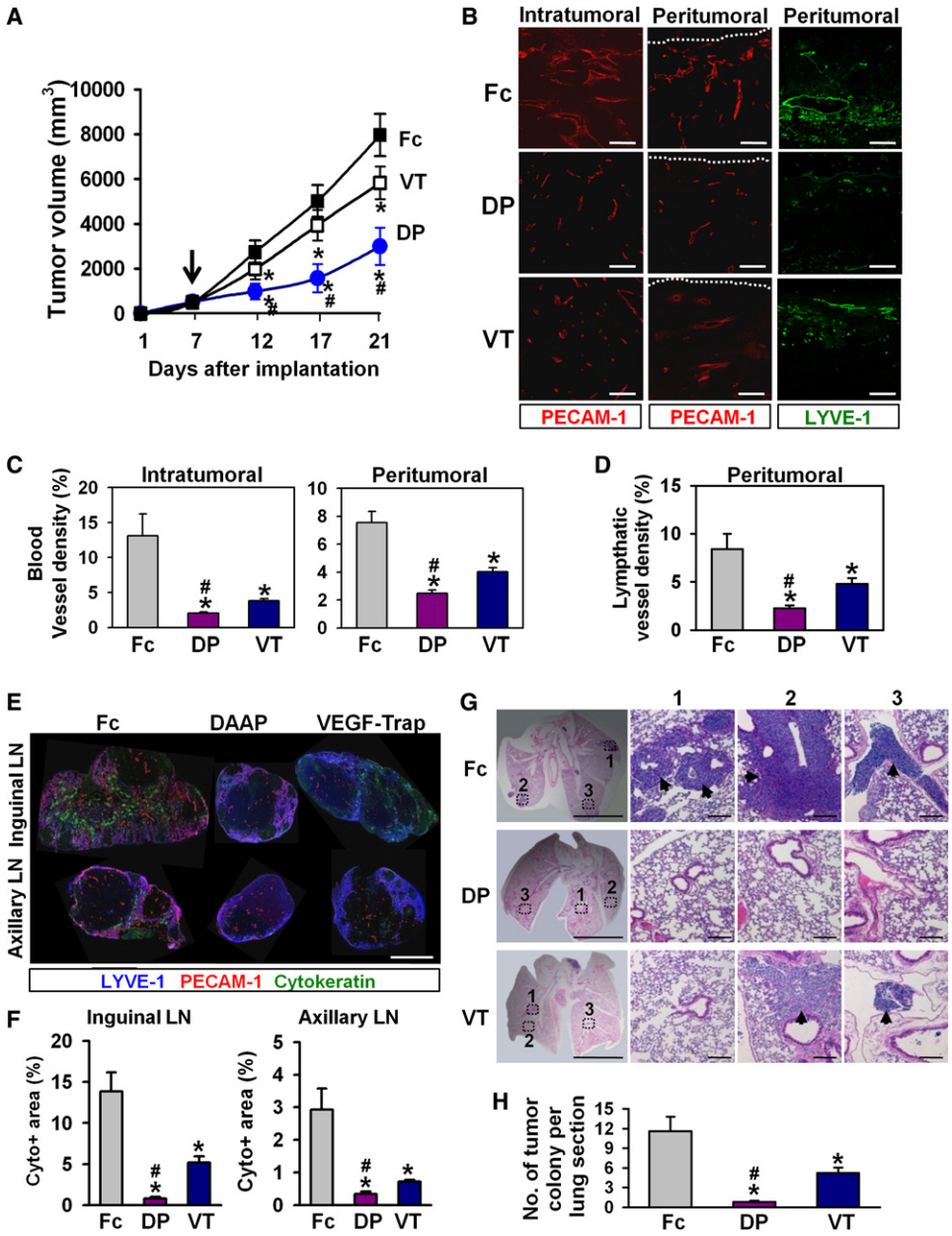


**Figure 3. DAAP Suppresses Tumor Growth, Vessel Formation, and Metastasis in Melanoma**

(A) Comparison of tumor growths. Each group, n = 5. *p < 0.05 versus Fc; #p < 0.05 versus VT. The arrow indicates the start of injections.

(B) Images showing PECAM-1+ blood vessels (red) and LYVE-1+ lymphatic vessels (green) in the peri- or intratumoral regions. White dotted-lines indicate the margin between the tumor and subcutaneous tissues. Scale bars represent 200 μm.

(C and D) The density of blood and lymphatic vessels in the peri- or intratumoral regions. Each group, n = 5. *p < 0.05 versus Fc; #p < 0.05 versus VT.

(E) Images showing the presence of cytokeratin+ melanoma cells in the inguinal LN (upper panel) and axillary LN (lower panel). Scale bars represent 1 mm.

(F) A comparison of the metastasis of cytokeratin+ melanoma cells in the LN. The area of cytokeratin+ fluorescence was presented as % per total sectioned area [Cyto+ area (%)]. Each group, n = 5. *p < 0.05 versus Fc; #p < 0.05 versus VT.

(G) Lung sections stained with H&E. Three regions of the lung sections (indicated in the left column) were viewed under high magnification. The arrows indicate clustered metastatic melanoma. Scale bars represent 5 mm (black) and 200 μm (white).

(H) Comparison of the number of melanoma colonies (>200 μm in diameter) in the lung sections. Each group, n = 5. *p < 0.05 versus Fc; #p < 0.05 versus VT.

DAAP and VEGF-Trap in additional tumor models. We generated an orthotopic colon cancer model by implanting 1 × $10^6$ CT-26-luc cells into the dome of the cecal wall of Balb/c mice (Figure S5). Seven days after implantation, the mice received subcutaneous injections of 25 mg/kg of Fc, VEGF-Trap, or DAAP every 2 days for the subsequent 3 weeks and the efficacy of antitumor effect were analyzed (Figure S5). We also used female MMTV-PyMT mice as a spontaneous breast tumor

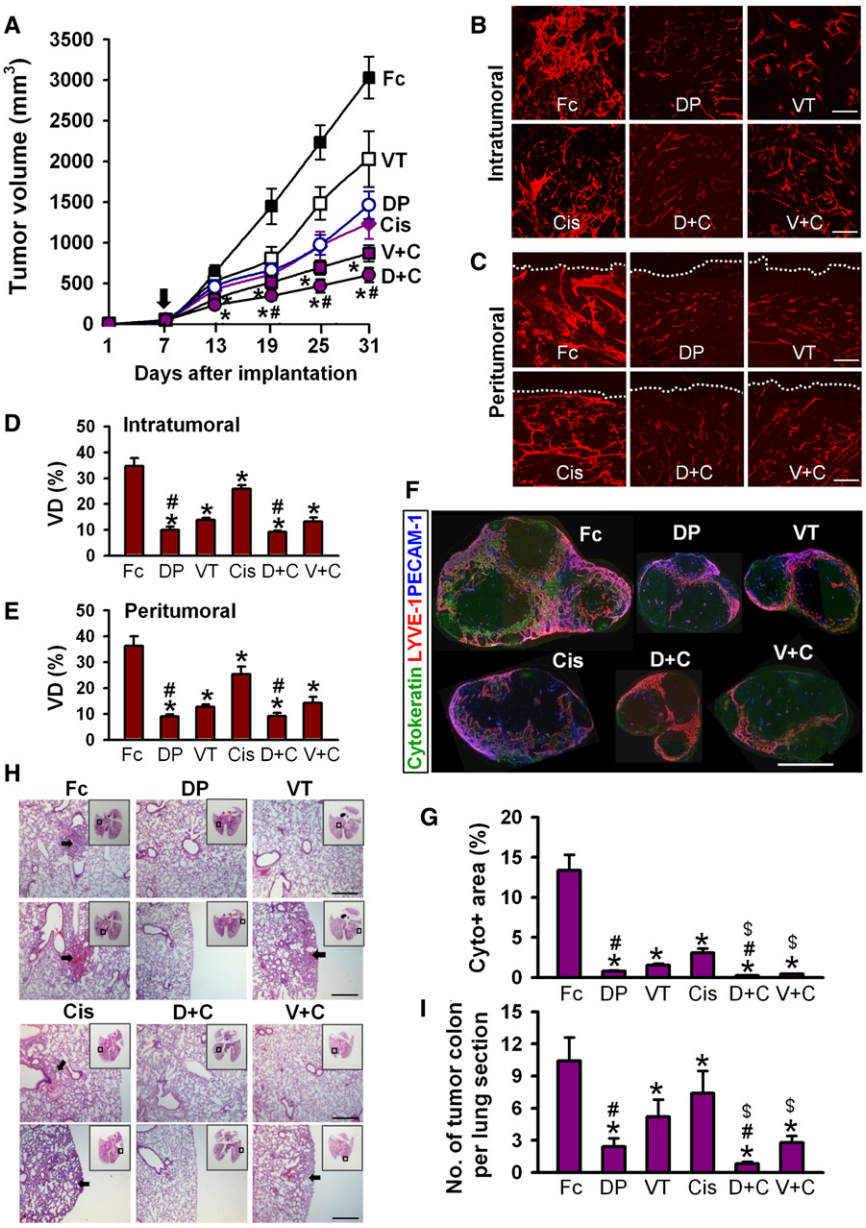


**Figure 4. Combination Therapy of DAAP Plus Cisplatin in Implanted LLC Tumors**

Seven days after LLC implantation, the mice were given injections of DAAP + cisplatin (D+C), VEGF-Trap + cisplatin (V+C), DAAP (DP), VEGF-Trap (VT), or dimeric-Fc (Fc). The proteins were given every 3 days and cisplatin was given every 7 days. Tissues were sampled on day 31.

(A) Comparison of tumor growths. Each group, n = 5. *p < 0.05 versus DP or VT; #p < 0.05 versus V+C. Arrow indicates the start of injections.

(B and C) Images showing PECAM-1+ blood vessels (red) in the intra- and peritumoral regions. White dotted lines indicate the margin between the tumor and subcutaneous tissues. Scale bars represent 200 μm.

(D and E) Densities of PECAM-1+ blood vessels (VD) in the intra- and peritumoral regions. Each group, n = 5. *p < 0.05 versus Fc; #p < 0.05 versus VT or V+C.

(F) Images showing the presence of cytokeratin+ LLC cells in the axillary LN. Scale bars represent 1 mm.

(G) Comparison of the metastasis of cytokeratin+ LLC cells in the axillary LN. The area of cytokeratin+ fluorescence was presented as % per total sectioned area [Cyto+ area (%)]. Each group, n = 5. *p < 0.05 versus Fc; #p < 0.05 versus VT or V+C; $p < 0.05 versus DP or VT.

(H) Lung sections stained with hematoxylin and eosin. Two regions of the lung sections (indicated as black lined square in each inset) were viewed under high magnification. The arrows indicate clustered metastatic LLC tumors. Scale bars represent 500 μm.

(I) Comparison of the number of tumor colonies (>200 μm in diameter) in the lung sections. Each group, n = 5. *p < 0.05 versus Fc; #p < 0.05 versus VT or V+C; $p < 0.05 versus DP or VT.

See also Figure S3.

model (Figure 6). At 10 weeks of age, the mice received subcutaneous injections of 25 mg/kg Fc, DAAP, or VEGF-Trap twice per week for the subsequent 5 weeks and the efficacy of antitumor effect were analyzed (Figure 6). In both tumor models, the growth, vascular density, and metastasis to the sentinel lymph node were significantly attenuated by DAAP and VEGF-Trap compared to Fc (Figure 6 and Figure S5). We noted that the effects of DAAP on the suppression of tumor growths, vascular densities, and metastasis to sentinel lymph node were significantly greater than those of VEGF-Trap in both tumor models (Figure 6 and Figure S5). However, enhanced invasion into the surrounding tissues was not detected in either tumor model at the end of the experiments (Figure 6B and Figure S5K).

## DAAP Reduces Vascular Leakage and Induces Tumor Vessel Normalization in Ovarian Carcinoma

To explore whether DAAP suppresses vascular leakage, we generated an orthotopic OVCA mouse model by implanting 3 × $10^7$ MDAH-2774 cells into athymic nude mice (Jeon et al., 2008). Seven days later, ~5 ml of ascites was aspirated from the mice, and the mice were given subcutaneous injections of 25 mg/kg DAAP or VEGF-Trap every 2 days for the subsequent week. Before sacrificing the mice, Evans blue and FITC-dextran were intravenously applied to examine vascular leakage in the peritoneal cavities. Both DAAP and VEGF-Trap markedly reduced ascites formation compared to Fc, but we noted that the ascites volume was 73% less by DAAP and 59% less by VEGF-Trap (Figures 7A and 7B). The Evans blue dye was markedly visible in the intestine and abdominal wall of the Fc-treated mice, but it was barely visible in the DAAP-treated mice and was mildly visible in VEGF-Trap treated mice (Figure 7C). In addition, the ascites of Fc-treated mice was

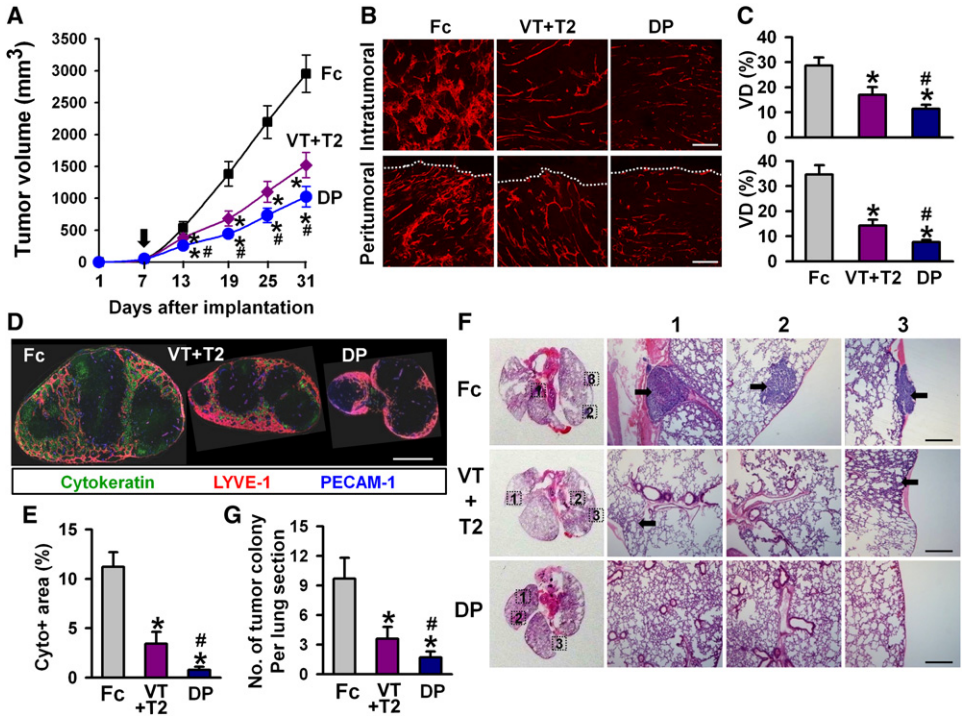


**Figure 5. DAAP Exerts Greater Antitumor Activities than Combined Therapy of VEGF-Trap and Tie2-Fc in Implanted LLC Tumor Model**

LLC implanted mice were given subcutaneous injections of DAAP (DP), VEGF-Trap + Tie2-Fc (VT+T2), or dimeric-Fc (Fc) every 3 days. Tissues were sampled 24 days after treatment.

(A) Comparison of tumor growths. Each group, n = 5. *p < 0.05 versus Fc; #p < 0.05 versus VT+T2. Arrow indicates the start of injections.

(B) Images showing PECAM-1+ blood vessels (red) in the intra- and peritumoral regions. White dotted lines indicate the margin between the tumor and subcutaneous tissues. Scale bars represent 200 μm.

(C) Densities of PECAM-1+ blood vessels (VD) in the intra- and peritumoral regions. Each group, n = 5. *p < 0.05 versus Fc; #p < 0.05 versus VT+T2.

(D) Images showing the presence of cytokeratin+ LLC cells in the axillary LN. Scale bar represents 1 mm.

(E) Comparison of the metastasis of cytokeratin+ LLC cells in the axillary LN. The area of cytokeratin+ fluorescence was presented as % per total sectioned area [Cyto+ area (%)]. Each group, n = 5. *p < 0.05 versus Fc; #p < 0.05 versus VT+T2.

(F) Lung sections stained with hematoxylin and eosin. Three regions of the lung sections (indicated as black lined squares) were viewed under high magnification. The arrows indicate clustered metastatic tumors. Scale bars represent 500 μm.

(G) Comparison of the number of tumor colonies (>200 μm in diameter) in the lung sections. Each group, n = 5. *p < 0.05 versus Fc; #p < 0.05 versus VT+T2. See also Figure S4.

highly hemorrhagic and contained a high level of Evans blue (304.6 ± 58.4 μg, n = 6), whereas the ascites DAAP-treated mice was mildly hemorrhagic and contained a low level of Evans blue (18.2 ± 3.7 μg, n = 6) and the ascites of mice treated with VEGF-Trap was moderately hemorrhagic and contained a moderate level of Evans blue (34.6 ± 5.2 μg, n = 6) (Figures 7D and 7E). The leakage measured by FITC-dextran was similar to that measured by Evans blue (Figures 7F and 7G), confirming that DAAP is superior to VEGF-Trap in preventing ascites formation in OVCA.

The dissemination and seeding of primary cancer cells onto organs in the peritoneal cavity, including the mesentery, is one of the characteristics of OVCA (Colombo et al., 2006). Consistent with this character, in this OVCA model, we observed the seeding and growing of tumors in the mesentery (Figure 7H). Compared to Fc treatment, disseminated tumor volume in the mesentery was 78% less by DAAP and 35% less by VEGF-Trap (Figures 7H and 7I). Confocal image analysis of the capillary beds in the mesenteric membranes revealed a robust increase of variably sized and tortuous vessels around the tumor area in untreated and Fc-treated mice, whereas the increase in abnormal capillary beds was moderate in the VEGF-Trap-treated mice and improperly developed and regressed capillary beds were observed around the micro-tumor area in DAAP-treated mice (Figure 7J). The capillary bed in the peritoneum of the abdominal wall showed that most capillaries were unorganized, dense, and chaotic in untreated and Fc-treated mice, whereas approximately 43% of capillary beds were normalized by VEGF-Trap and 57% by DAAP. Interestingly, the DAAP-treated capillary beds were less enlarged and more organized than the VEGF-Trap-treated capillary beds (Figure 7K). Moreover, the DAAP-treated mice displayed more well-arranged PECAM-1 distribution in the junction region of the endothelium in the peritoneum of the abdominal wall and more ghost vessels (CD31−/collagen IV+; Inai et al., 2004) in the mesenteric membrane than in the VEGF-Trap-treated mice (Figure S6). Furthermore, we found that MDAH-2774 cell implantation caused a robust induction of host Ang-2 in the abdominal

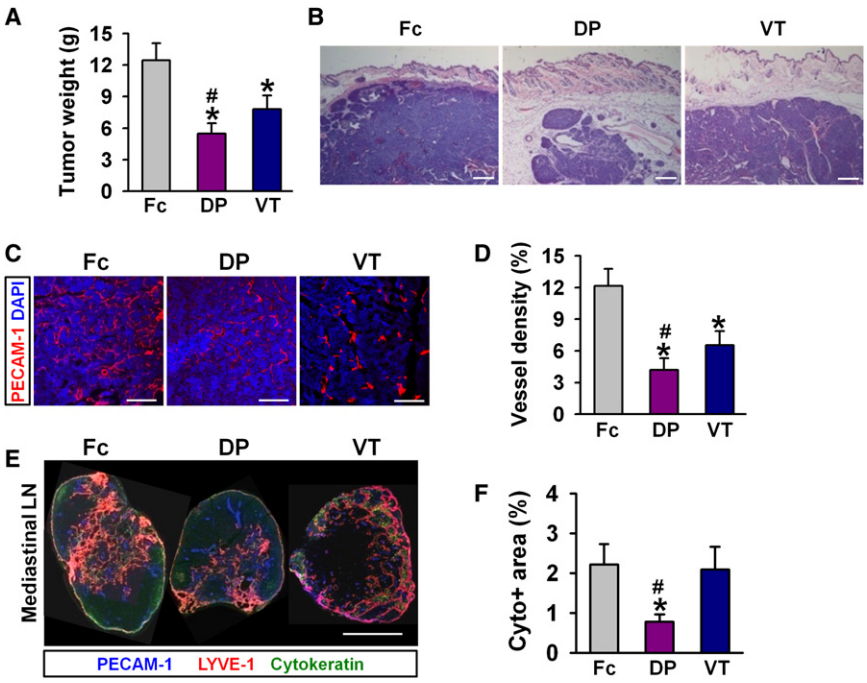


**Figure 6. DAAP Reduces Tumor Growth, Vessel Formation, and Metastasis in Spontaneous Breast Tumor Model**

(A) Comparison of dissected tumor weight. Each group, n = 4. *p < 0.05 versus Fc; #p < 0.05 versus VT.

(B) Tumor sections stained with hematoxylin and eosin. Scale bars represent 250 μm.

(C) Images showing PECAM-1$^+$ blood vessels (red) in tumors. Scale bars represent 200 μm.

(D) Densities of PECAM-1$^+$ blood vessels in tumors. Each group, n = 4. *p < 0.05 versus Fc; #p < 0.05 versus VT.

(E) Images showing the presence of cytokeratin$^+$ breast cancer cells in the mediastinal LN. Scale bar represents 1 mm.

(F) Comparison of the metastasis of cytokeratin$^+$ breast cancer cells in the mediastinal LN. The area of cytokeratin$^+$ fluorescence was presented as % per total sectioned area [Cyto$^+$ area (%)]. Each group, n = 4. *p < 0.05 versus Fc; #p < 0.05 versus VT.

See also Figure S5.

organs, including the mesentery (Figure 8A). Thus, DAAP is more effective than VEGF-Trap in preventing vascular leakage, tumor dissemination, and progression, and the induction of aberrant capillary bed normalization most likely occurs via tumor- and host-derived VEGF-A and Ang-2 in OVCA.

### Close Correlation between DAAP Efficacy and Expression of VEGF-A and Ang-2 in the Tumor Models

The aforementioned findings led us to determine how DAAP acted dominantly over VEGF-Trap on its target in the tumor models. Quantitative RT-PCR analyses revealed that the levels of VEGF-A, VEGFR2, Ang-2, and Tie2 mRNA were markedly upregulated in endothelial cells of the growing tumors (2 weeks after implantation of LLC or B16/F10 cells) compared to nonendothelial cells or adjacent normal tissues (Table S2). In contrast, the level of Ang-1 mRNA was not changed in either the endothelial cells or nonendothelial cells of the growing tumor (Table S2). Thus, there were close co-relationships between DAAP efficacy and the expression of VEGF-A, VEGFR2, Ang-2, and Tie2, but there was no relationship between DAAP efficacy and Ang-1 expression. We also examined the distribution of VEGFR2, Ang-2, and Tie2 in the tumors by immunohistochemistry and using a genetically-modified mouse (heterozygous Ang-2$^{+/LacZ}$) (Gale et al., 2002) (Figure 8). All of the results obtained from immunohistochemistry and the Ang-2$^{+/LacZ}$ mice correlated well with the data obtained from quantitative RT-PCR (Figure 8). Furthermore, Ang-2 mRNA levels were upregulated robustly by VEGF-Trap and moderately by DAAP in the tumors (Table S3). In contrast, even during treatment with DAAP or VEGF-Trap, Ang-1 mRNA levels were not upregulated in the tumor tissues (Table S3). Given these results, the efficacy of DAAP seems to largely depend on the inhibition of Ang-2, in addition to VEGF-A, rather than Ang-1 in the tumors.

## DISCUSSION

In this study, we developed what we believe to be a DAAP that simultaneously blocks VEGF-A/PlGF and angiopoietin. Although the affinity of DAAP for VEGF-A is roughly three times lower than its affinity for VEGF-Trap, it could be within the 5–10 pM range, which is quite high compared to other decoy receptors and antibodies against VEGF-A. However, the affinity of DAAP for Ang-2 is roughly five times higher than that of Tie2-Fc. Furthermore, the binding of VEGF-A or Ang-2 to DAAP enhances its binding of Ang-2 or VEGF-A, respectively, and could be a supplementary benefit of using DAAP to block VEGF-A and Ang-2. Bioavailability is of paramount importance in the systemic use of bioactive molecules and developing therapeutic proteins. DAAP has relatively high bioavailability and a longer half-life than VEGF-Trap, raising the possibility that DAAP could be a superior therapeutic protein to VEGF-Trap, assuming that it retained its ability to simultaneously bind and block VEGF-A and angiopoietins. Indeed, in suppressing tumor growth, angiogenesis, and metastasis, DAAP was superior to the combined therapy of VEGF-Trap plus Tie2-Fc, and DAAP was also superior to VEGF-Trap when in combination with cytotoxic chemotherapy agents such as cisplatin and dacarbazine. Based on these results, we propose that the simultaneous blockade of VEGF-A and Ang by DAAP can be an effective therapeutic strategy for blocking tumor angiogenesis, metastasis, and vascular leakage. Nevertheless, repeated DAAP treatment induced anticipated toxicities such as thrombocytosis, hypertension and microalbuminuria and seem to correlate with the extent of endogenous VEGF-A blockade (Lockhart et al., 2010; Tam et al., 2006; Verheul and Pinedo, 2007). However, repeated administration of DAAP did not generate autoantibodies to new epitopes created at the junctions of elements from the different proteins

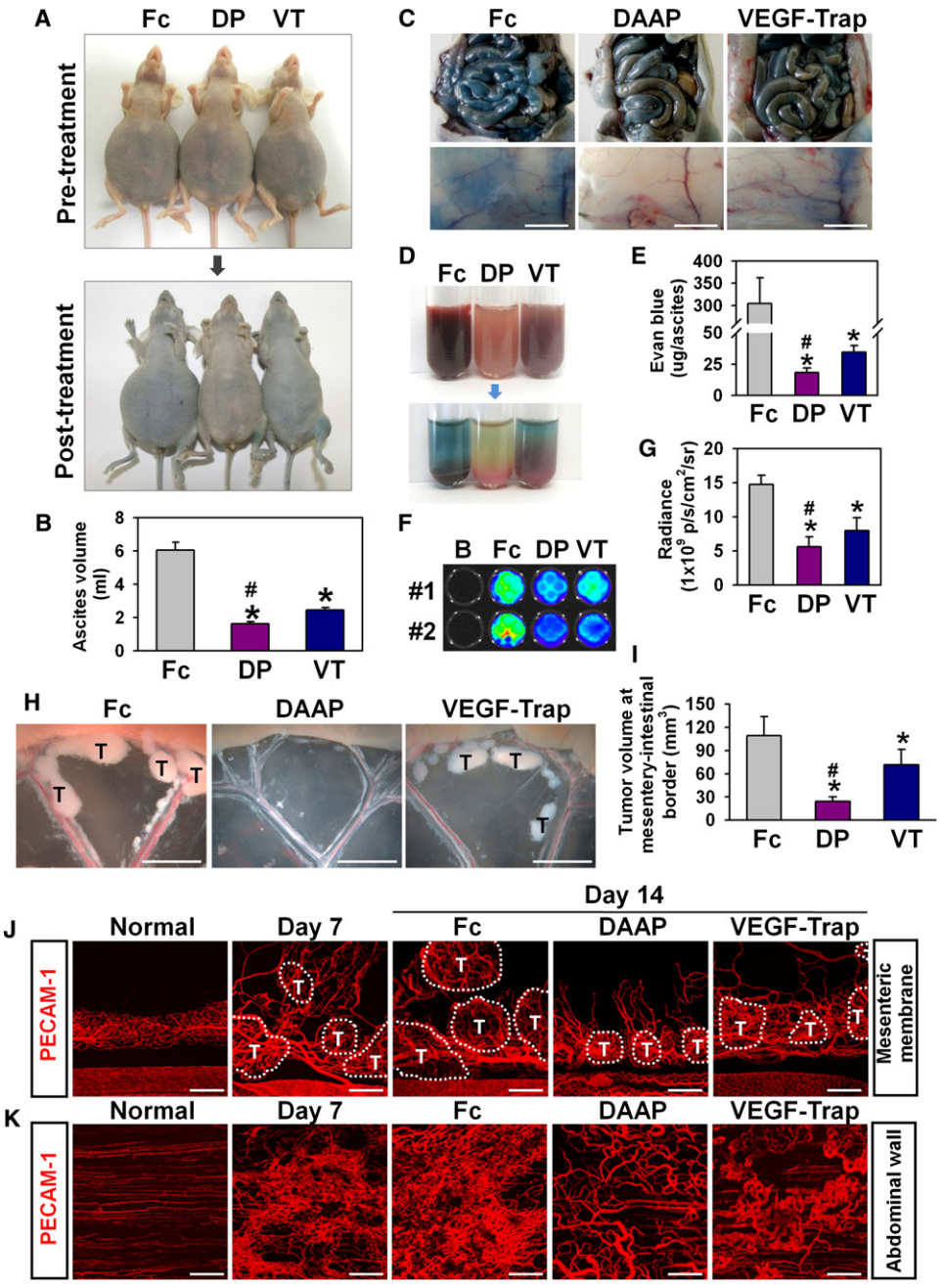


**Figure 7. DAAP Reduces Ascites Formation in OVCA**

(A) Photographs showing the gross features of ascites formation on day 7 (upper panel) and 14 (lower panel) after MDAH-2774 cell implantation.

(B) Comparison of ascites volume. Each group, n = 5. *p < 0.05 versus Fc.

(C) Photographs showing Evans blue dye leakage in the intestines and abdominal walls. Scale bars represent 5 mm.

(D) Photographs showing the aspirated ascites before (upper panel) and after (lower panel) centrifugation. The red color indicates red blood cells, whereas the blue color indicates Evans blue dye.

(E) Comparison of Evans blue amounts in the ascites. Each group, n = 5. *p < 0.05 versus Fc.

(F) Photographs showing FITC-dextran in 20 μl of ascites in two examples (1 and 2). B: blank well.

(G) Quantification of FITC-dextran in the ascites, expressed as radiance (photon/sec/cm$^2$/steradian). Each group, n = 5. *p < 0.05 versus Fc.

(H) Photograph showing the gross features of tumor growth along the mesentery-intestinal border. T: tumor. Scale bars represent 5 mm.

(I) Comparison of tumor volume along the mesentery-intestinal border. Each group, n = 5. *p < 0.05 versus Fc; #p < 0.05 versus VT.

(J and K) Immunostaining micrographs for PECAM-1 showing the patterns of blood vessels in the peritoneum of the anterior mesenteric membrane and abdominal wall. Normal, untreated normal mouse; Day 7 and 14, time after MDAH-2774 cell transplantation. T: tumor regions on the mesenteric membrane. Scale bars represent 200 μm.

See also Figure S6.

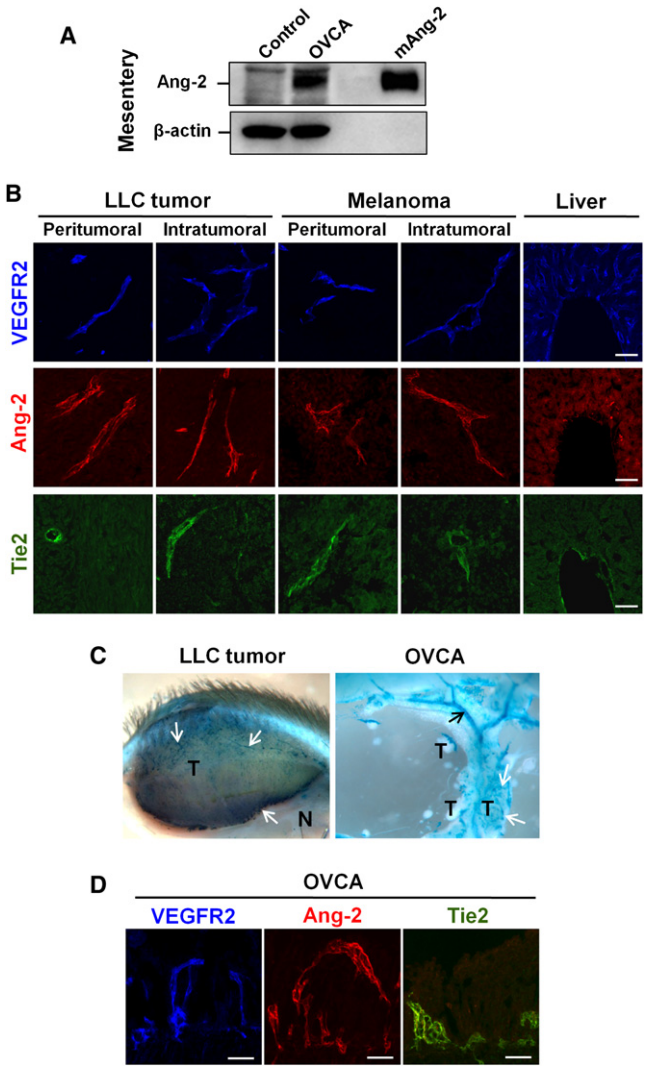


**Figure 8. Close Correlation between DAAP Efficacy and Expression of VEGF-A and Ang-2 in the Tumor Models**

(A) Seven days after MDAH-2774 cell implantation (OVCA) or PBS injection (Control) into athymic nude mice, the mesenteries were sampled. Tissue lysates (100 μg of protein) and 100 ng of recombinant mouse Ang-2 were analyzed by immunoblotting using an antimouse Ang-2 antibody. The membrane was stripped and reprobed with anti-β-actin antibody. Three independent experiments showed similar findings.

(B) Immunohistochemical localization of VEGFR2, Ang-2 and Tie2 in the intra- and peritumoral regions 2 weeks after tumor cells implantation, liver was used as a control. Scale bars represent 100 μm. Note that these are highly expressed in tumor blood vessels.

(C) Ang-2 expression in implanted LLC and OVCA tumors in the Ang-$2^{+/LZ}$ mice. Strong expression of Ang-2 (dark blue) is detected in tumor blood vessels (white arrows) and mesenteric vessels (black arrow). In comparison, expression of Ang-2 is strongly detected in the large-sized, but not in small-sized mesenteric vessels, in normal condition. N: normal region; T: tumor.

(D) Immunohistochemical localization of Ang-2 and Tie2 in the OVCA tumor. Scale bars represent 100 μm. Note that these are highly expressed in the peritoneal blood vessels.

See also Tables S2 and S3.

or to the targeting receptors in this treatment regime. Therefore, like other soluble receptors and therapeutic antibodies, DAAP is unlikely to be an immunogenic protein.

These promising outcomes raise several intriguing questions. First, what are the advantages of DAAP over combined therapy with VEGF-Trap and Tie2-Fc and does DAAP have equivalent benefits to the engineered fusion antibodies that contain more than two binding sites (Wu et al., 2007)? Each protein has a different biodistribution and half-life, which are sometimes critical factors for effectiveness in anticancer therapy. DAAP appeared to distribute well in the tumor environment and block VEGF-A and Ang-2 in a synergistic manner, possibly with increased ligand aggregation due to increased avidity effect (Nowakowski et al., 2002). In contrast, because VEGF-Trap and Tie2-Fc have different biodistributions and half-lives in the body, they could not produce synergistic effects in the tumor environment. Moreover, DAAP has a longer half-life than VEGF-Trap and Tie2-Fc. A single anticancer agent could be more cost-effective than dual anticancer agents. In this regard, DAAP could have benefits equivalent to the engineered fusion antibody.

Second, do all tumors highly express both VEGF-A/VEGFR2 and Ang/Tie2 systems, and are they activated in growing metastatic tumors? If so, is it worthwhile to block both systems to effectively suppress tumor angiogenesis and metastasis? Accumulating evidence (Augustin et al., 2009; Ferrara and Kerbel, 2005; Folkman, 2007; Huang et al., 2009; Shim et al., 2007), including our findings, indicates that most tumors in human patients and experimental animal models have high expression and activation levels of both VEGF-A/VEGFR2 and Ang/Tie2 and that these systems produce interactive synergistic effects on tumor angiogenesis and metastasis. In particular, consistent with our findings, numerous evidences indicate that Ang-2, not Ang-1, is a major angiopoietin protein for enhancing tumor angiogenesis along with several growth factors, including VEGF-A. A recent report indicates that host-derived Ang-2 affects early tumor angiogenesis, although it may be dispensable for later tumor angiogenesis (Nasarre et al., 2009). Moreover, our study showed that Ang-1 expression was not changed in the growing tumor and even during treatment with DAAP or VEGF-Trap. Tie2 signaling may also act directly on tumor cells in a paracrine and autocrine manner; the receptor is being found increasingly in tumor cells (Martin et al., 2008). Collectively, it is worthwhile to doubly block angiopoietins in addition to VEGF-A/PlGF to reduce tumor angiogenesis and metastasis. Meeting this expectation and consistent with recent reports (Brown et al., 2010; Hashizume et al., 2010), our results show that double and simultaneous blockade of these ligands using DAAP is highly effective in suppressing tumor angiogenesis and metastasis compared to the single blockade of VEGF-A/PlGF or Ang.

A third question is why DAAP is more effective than VEGF-Trap in preventing vascular leakage in the OVCA mouse model. VEGF-A is the primary molecule responsible for producing ascites in OVCA, inducing vascular permeability in peritoneal microvessels (Nagy et al., 1995). Ang-2 could be an additional factor for the induction of ascites formation, enhancing the destabilization and leakage of the peritoneal microvessels (Parikh et al., 2006; Zhang et al., 2003). Our results suggest that

Ang-2 might be derived from host cells, and not from growing OVCA cells. Zhang et al. (2003) showed that OVCA-derived VEGF-A upregulates Ang-2 in host endothelial cells, which could result in further destabilization and leakage of the host vasculature surrounding the tumors and peritoneum. Indeed, formation of the unorganized, dense, and chaotic capillaries is prevalent in the peritoneum of the abdominal wall in OVCA mice, which is responsible for severe vascular leakage and ascites formation. Given these changes in OVCA, our data suggest that the greater anti-leak action of DAAP compared to VEGF-Trap may be partly due to (1) enhanced normalization of tumor vessel (Jain, 2003); (2) greater reduction in the unorganized, dense, and chaotic vascular surface area due to tumor vessel pruning; (3) more generalized improvement in endothelial barrier function; and (4) less formation of ascites. Although DAAP could be considered to disrupt the anti-leakage actions of Ang-1, the Ang-1 level for counteracting Ang-2 was negligible in the OVCA mice. Therefore, we strongly believe that the double blockade of VEGF-A and Ang-2 with DAAP is more effective at preventing the formation of ascites in the OVCA mouse model than the single blockade of VEGF-A by VEGF-Trap.

Fourth, could DAAP suppress the increased local invasion and accelerated metastasis in anti-VEGF-A therapy-elicited malignant tumor progression? In contrast to the largely known concept, the blockade of VEGF-A-VEGFR2 signaling reduces primary tumor growth but promotes tumor invasiveness and metastasis. The increased expression of other proangiogenic factors, including Ang-1, Ang-2, and fibroblast growth factors, a process termed angiogenic rescue (Casanovas et al., 2005) could be a main underlying mechanism for this phenomenon. These findings reflect challenging clinical outcomes derived from the single antiangiogenic therapy, such as only a short-term delay of survival rate, adaptive resistance, intrinsic nonresponsiveness, and the rapid re-growth of tumor vessels after ceasing therapy (Bergers and Hanahan, 2008; Mancuso et al., 2006). This fact was recently highlighted in reports (Ebos et al., 2009; Loges et al., 2009; Paez-Ribes et al., 2009). Combined therapy for antiangiogenesis and antiproliferation is expanding experimentally in various cancer models and clinically in numerous types of cancer patients. In this regard, it should be noted that angiopoietins could be one of the main factors for inducing tumor re-growth, adaptive resistance, and accelerated metastasis during VEGF-A-VEGFR2 blockade (Huang et al., 2009). In this scenario, DAAP could be a potential agent for suppressing the anti-VEGF-A therapy-elicited malignant tumor progression.

Finally, there could be possible shortcomings of DAAP compared to VEGF-Trap or specific anti-Ang-2 blocking antibody, such as (1) blocking the beneficial or antitumor effects of Ang-1; (2) slower production rate in mammalian cells; (3) no advantage in solely VEGF-A-dependent nontumor diseases; or 4) no advantage in Ang-2-dependent tumor and nontumor diseases. If one could develop an alternative DAAP variant that selectively blocks VEGF-A and Ang-2, it could avoid the problem of blocking the beneficial effect of Ang-1. However, we believe our findings clearly indicate that tumor angiogenesis is mainly dependent on both VEGF-A and Ang-2, not on Ang-1, in the tumors we studied. Therefore, the application of DAAP deserves to be diversified to various tumor models to determine the possible benefits and effectiveness over VEGF-Trap.

In conclusion, DAAP is a chimeric decoy receptor that can bind and block both VEGF-A and angiopoietins. By virtue of this advantage, DAAP exhibits marked effectiveness in suppressing the tumor angiogenesis and metastasis of implanted and spontaneous solid tumors and in reducing ascites formation and vascular leakage in advanced OVCA. Further preclinical studies are warranted to explore additional applications of DAAP for the control of pathologic angiogenesis, including anti-VEGF-A therapy-elicited local invasion and metastasis.

## EXPERIMENTAL PROCEDURES

### Measurement of Toxicity

Six-week-old male C57BL/6J mice (~17 g body weight) were given subcutaneous injections of PBS, 25 mg/kg of Fc, VEGF-Trap, DAAP, or Tie2-Fc recombinant protein every 3 days for 30 days. One day after the last treatment, systolic blood pressure and heart rate were measured by an automated tail-cuff device (IITC Life Science) under conscious state in a restrainer. Two days after the last treatment, blood and urine samples were collected. Hematocrit was measured by a hemocytometer (Heamatokrit 210, Hettich), WBC and differential counts of WBC were measured by an automated CBC counter (VetScan HM5 Hematology, ABXIS), and chemical analyses for blood and urine were performed by a chemistry analyzer (VetTest 8008, IDEXX Laboratories Inc.). Urinary albumin was measured by an immunoperoxidase assay using The Albumin test kit according to the manufacturer's instruction (GenWay Biotech).

### Generation of Tumor Models and Treatment Regimes

Specific pathogen-free C57BL/6J, Balb/C, MMTV-PyMT transgenic mice (FVB/N), and BALB/cByJ athymic nude (CbyJ.Cg-*Foxn1*$^{nu}$/J) were purchased from Jackson Laboratory. All animals were bred in our pathogen-free animal facility. Animal care and experimental procedures were performed with the approval of the Animal Care Committee of KAIST. In particular, we performed the melanoma experiments with special permission from the committee and were allowed to grow the tumor until it reached 30% of the body weight to assess the extent of metastasis to the lung.

Mouse LLC, B16/F10 melanoma, CT-26, and human MDAH-2774 ovarian cancer cell lines were obtained from the American Type Culture Collection. CT-26 cells (Balb/c background) were transduced with the *luciferase* gene by a retroviral transfer, selected as a colony, and termed as "CT-26-luc" cells (Dr. Kyung Keun Kim, Chonnam University, Korea).

To generate an implantation tumor model, a suspension ($1 \times 10^6$ cells in 100 μl) of LLC or B16/F10 cells were subcutaneously implanted into the flank region of C57BL/6J mice and a suspension ($1 \times 10^6$ cells in 100 μl) of CT-26-luc cells was orthotopically implanted into the dome of the cecal wall of Balb/c mice. Indicated days later, the mice were given subcutaneous injections of DAAP, VEGF-Trap, Tie2, or dimeric-Fc (indicated dose, frequency, and duration). As a control, an equal volume of PBS was injected in the same manner. Indicated days later, the mice were anesthetized by intramuscular injection of 80 mg/kg ketamine and 12 mg/kg xylazine, tumor volumes were measured, and primary tumors, indicated lymph nodes, lungs, and livers were harvested for histological analyses. To administer a chemotherapeutic agent to the LLC tumor model, intraperitoneal injections of cisplatin (10 mg/kg every 7 days; Sigma-Aldrich) were performed 7 days after tumor implantation. To administer a chemotherapeutic agent to the melanoma model, a treatment cycle consisted of an intraperitoneal injection of dacarbazine (20 mg/kg; Sigma-Aldrich) followed by an epifocal application of dinitrochlorobenzene (dissolved in a 4:1 mixture of acetone and olive oil) on the tumor 7 days after tumor implantation. For the first cycle, the tumors were treated with 2% dinitrochlorobenzene, whereas for the following cycles 1% dinitrochlorobenzene was used. Cycles were repeated every 4 days. To compare the effect of DAAP on the established LLC tumor, 14 days after implantation, the mice with equal sized (~500 $mm^3$) tumors were chosen.

To generate an advanced OVCA model, a suspension of MDAH-2774 cells ($3 \times 10^7$ in 500 μl PBS) was injected into the peritoneal cavity of female nude mice (Jeon et al., 2008). Seven days after injection, ~5 ml of ascites

was aspirated from the mice, and the mice were given four subcutaneous injections of DAAP, VEGF-Trap, or dimeric-Fc (25 mg/kg) at every 2 days.

Heterozygous Ang-$2^{+/LacZ}$ mice (C57/BL/6J) were kindly provided by Regeneron Pharmaceuticals. Mouse ovarian carcinoma cell line, ID-8 (C57BL/6J background), was kindly provided by Dr. Kathy Roby (University of Kansas Medical Center). The cell lines were cultured in DMEM (GIBCO BRL) containing 10% heat-inactivated FBS (HyClone), penicillin, and streptomycin (Sigma-Aldrich) in plastic tissue culture dishes (Nunc) at 37°C in a humidified atmosphere of 5% $CO_2$. To examine Ang-2 gene expression in tumors, LLC cells ($1 \times 10^6$ in 100 μl PBS) were subcutaneously implanted into the flank region of Ang-$2^{+/LacZ}$ mice or ID-8 cells ($1 \times 10^7$ in 500 μl PBS) were intraperitoneally implanted into Ang-$2^{+/LacZ}$ mice.

### Vascular Leakage Assay in the OVCA model

Indicated days after MDAH-2774 cell implantation for generation of OVCA model, the mice were anesthetized and administered Evans blue (80 mg/kg) or 100 μl FITC-dextran (43,200 Da, 500 mg/ml) via the infraorbital plexus veins to measure vascular permeability in the peritoneal cavities. Forty minutes after the dye injection, the ascites was aspirated, its volume measured, and the sample centrifuged at 14,000 × *g*. The Evans blue concentration in the ascites was measured with a spectrophotometer using a Perkin-Elmer multi-plate reader at 595 nm (Wallac Victor$^2$V, Perkin-Elmer), and the fluorescence intensity of FITC-dextran in the ascites was quantified in 50 μl of ascites from each mouse using Living Image software (Xenogen) and expressed as radiance (photon/sec/cm$^2$/steradian).

### Statistics

Values are presented as mean ± standard deviation (SD). Significant differences between means were determined by an analysis of variance followed by the Student-Newman-Keuls test. Statistical significance was set at $p < 0.05$.

Additional experimental procedures, including generation of recombinant proteins, ELISA, surface plasmon resonance assay, deglycosylation assay, in vitro pull down assay, ECM binding assay, measurement of the pI value, phosphorylation assay, inhibition assay for endothelial cell proliferation, pharmacokinetic analysis, luminographic imaging of tumor size, histological and morphometric analysis, and endothelial cell sorting and quantitative real-time PCR, are listed in the Supplemental Experimental Procedures.

## SUPPLEMENTAL INFORMATION

Supplemental Information includes six figures, three tables, and Supplemental Experimental Procedures and can be found with this article online at doi:10.1016/j.ccr.2010.07.001.

## ACKNOWLEDGMENTS

We thank Jin Sun Hong and Eun Soon Lee for their technical assistance, Dr. N. Gale for Ang-$2^{+/LacZ}$ mice, Dr. K.K. Kim for CT-26-luc cells, Dr. K. Roby for ID-8 cells, and Dr. Rolf Brekken for anti-VEGFR2 antibody. This work was supported by the Korea Science and Engineering Foundation (KOSEF) funded by the MEST (R2009-0079390 and R31-2009-000-10071-0 to G.Y.K.) and the Korea Healthcare Technology R&D Project, Ministry for Health, Welfare and Family Affairs, Korea (A092255 to G.Y.K.).

Received: May 29, 2009
Revised: April 5, 2010
Accepted: July 12, 2010
Published: August 16, 2010

## REFERENCES

Ahmad, S.A., Liu, W., Jung, Y.D., Fan, F., Wilson, M., Reinmuth, N., Shaheen, R.M., Bucana, C.D., and Ellis, L.M. (2001). The effects of angiopoietin-1 and −2 on tumor growth and angiogenesis in human colon cancer. Cancer Res. *61*, 1255–1259.

Augustin, H.G., Koh, G.Y., Thurston, G., and Alitalo, K. (2009). Control of vascular morphogenesis and homeostasis through the angiopoietin-Tie system. Nat. Rev. Mol. Cell Biol. *10*, 165–177.

Bergers, G., and Hanahan, D. (2008). Modes of resistance to anti-angiogenic therapy. Nat. Rev. Cancer *8*, 592–603.

Brown, J.L., Cao, Z.A., Pinzon-Ortiz, M., Kendrew, J., Reimer, C., Wen, S., Zhou, J.Q., Tabrizi, M., Emery, S., McDermott, B., et al. (2010). A human monoclonal anti-ANG2 antibody leads to broad antitumor activity in combination with VEGF inhibitors and chemotherapy agents in preclinical models. Mol. Cancer Ther. *9*, 145–156.

Byrne, A.T., Ross, L., Holash, J., Nakanishi, M., Hu, L., Hofmann, J.I., Yancopoulos, G.D., and Jaffe, R.B. (2003). Vascular endothelial growth factor-trap decreases tumor burden, inhibits ascites, and causes dramatic vascular remodeling in an ovarian cancer model. Clin. Cancer Res. *9*, 5721–5728.

Casanovas, O., Hicklin, D.J., Bergers, G., and Hanahan, D. (2005). Drug resistance by evasion of antiangiogenic targeting of VEGF signaling in late-stage pancreatic islet tumors. Cancer Cell *8*, 299–309.

Colombo, N., Van Gorp, T., Parma, G., Amant, F., Gatta, G., Sessa, C., and Vergote, I. (2006). Ovarian cancer. Crit. Rev. Oncol. Hematol. *60*, 159–179.

Davis-Smyth, T., Chen, H., Park, J., Presta, L.G., and Ferrara, N. (1996). The second immunoglobulin-like domain of the VEGF tyrosine kinase receptor Flt-1 determines ligand binding and may initiate a signal transduction cascade. EMBO J. *15*, 4919–4927.

Ebos, J.M., Lee, C.R., Cruz-Munoz, W., Bjarnason, G.A., Christensen, J.G., and Kerbel, R.S. (2009). Accelerated metastasis after short-term treatment with a potent inhibitor of tumor angiogenesis. Cancer Cell *15*, 232–239.

Falcon, B.L., Hashizume, H., Koumoutsakos, P., Chou, J., Bready, J.V., Coxon, A., Oliner, J.D., and McDonald, D.M. (2009). Contrasting actions of selective inhibitors of angiopoietin-1 and angiopoietin-2 on the normalization of tumor blood vessels. Am. J. Pathol. *175*, 2159–2170.

Ferrara, N., and Kerbel, R.S. (2005). Angiogenesis as a therapeutic target. Nature *438*, 967–974.

Ferrara, N., Hillan, K.J., Gerber, H.P., and Novotny, W. (2004). Discovery and development of bevacizumab, an anti-VEGF antibody for treating cancer. Nat. Rev. Drug Discov. *3*, 391–400.

Folkman, J. (2007). Angiogenesis: an organizing principle for drug discovery? Nat. Rev. Drug Discov. *6*, 273–286.

Gale, N.W., Thurston, G., Hackett, S.F., Renard, R., Wang, Q., McClain, J., Martin, C., Witte, C., Witte, M.H., Jackson, D., et al. (2002). Angiopoietin-2 is required for postnatal angiogenesis and lymphatic patterning, and only the latter role is rescued by Angiopoietin-1. Dev. Cell *3*, 411–423.

Hashizume, H., Falcon, B.L., Kuroda, T., Baluk, P., Coxon, A., Yu, D., Bready, J.V., Oliner, J.D., and McDonald, D.M. (2010). Complementary Actions of Inhibitors of Angiopoietin-2 and VEGF on Tumor Angiogenesis and Growth. Cancer Res. *70*, 2213–2223.

Holash, J., Maisonpierre, P.C., Compton, D., Boland, P., Alexander, C.R., Zagzag, D., Yancopoulos, G.D., and Wiegand, S.J. (1999). Vessel cooption, regression, and growth in tumors mediated by angiopoietins and VEGF. Science *284*, 1994–1998.

Holash, J., Davis, S., Papadopoulos, N., Croll, S.D., Ho, L., Russell, M., Boland, P., Leidich, R., Hylton, D., Burova, E., et al. (2002). VEGF-Trap: a VEGF blocker with potent antitumor effects. Proc. Natl. Acad. Sci. USA *99*, 11393–11398.

Huang, J., Bae, J.O., Tsai, J.P., Kadenhe-Chiweshe, A., Papa, J., Lee, A., Zeng, S., Kornfeld, Z.N., Ullner, P., Zaghloul, N., et al. (2009). Angiopoietin-1/Tie-2 activation contributes to vascular survival and tumor growth during VEGF blockade. Int. J. Oncol. *34*, 79–87.

Hurwitz, H., Fehrenbacher, L., Novotny, W., Cartwright, T., Hainsworth, J., Heim, W., Berlin, J., Baron, A., Griffing, S., Holmgren, E., et al. (2004). Bevacizumab plus irinotecan, fluorouracil, and leucovorin for metastatic colorectal cancer. N. Engl. J. Med. *350*, 2335–2342.

Inai, T., Mancuso, M., Hashizume, H., Baffert, F., Haskell, A., Baluk, P., Hu-Lowe, D.D., Shalinsky, D.R., Thurston, G., Yancopoulos, G.D., and McDonald, D.M. (2004). Inhibition of vascular endothelial growth factor (VEGF)

signaling in cancer causes loss of endothelial fenestrations, regression of tumor vessels, and appearance of basement membrane ghosts. Am. J. Pathol. *165*, 35–52.

Jain, R.K. (2003). Molecular regulation of vessel maturation. Nat. Med. *9*, 685–693.

Jeon, B.H., Jang, C., Han, J., Kataru, R.P., Piao, L., Jung, K., Cha, H.J., Schwendener, R.A., Jang, K.Y., Kim, K.S., et al. (2008). Profound but dysfunctional lymphangiogenesis via vascular endothelial growth factor ligands from CD11b+ macrophages in advanced ovarian cancer. Cancer Res. *68*, 1100–1109.

Lockhart, A.C., Rothenberg, M.L., Dupont, J., Cooper, W., Chevalier, P., Sternas, L., Buzenet, G., Koehler, E., Sosman, J.A., Schwartz, L.H., et al. (2010). Phase I study of intravenous vascular endothelial growth factor trap, aflibercept, in patients with advanced solid tumors. J. Clin. Oncol. *28*, 207–214.

Loges, S., Mazzone, M., Hohensinner, P., and Carmeliet, P. (2009). Silencing or fueling metastasis with VEGF inhibitors: antiangiogenesis revisited. Cancer Cell *15*, 167–170.

Macdonald, P.R., Progias, P., Ciani, B., Patel, S., Mayer, U., Steinmetz, M.O., and Kammerer, R.A. (2006). Structure of the extracellular domain of Tie receptor tyrosine kinases and localization of the angiopoietin-binding epitope. J. Biol. Chem. *281*, 28408–28414.

Mancuso, M.R., Davis, R., Norberg, S.M., O'Brien, S., Sennino, B., Nakahara, T., Yao, V.J., Inai, T., Brooks, P., Freimark, B., et al. (2006). Rapid vascular regrowth in tumors after reversal of VEGF inhibition. J. Clin. Invest. *116*, 2610–2621.

Martin, V., Liu, D., Fueyo, J., and Gomez-Manzano, C. (2008). Tie2: a journey from normal angiogenesis to cancer and beyond. Histol. Histopathol. *23*, 773–780.

Nagy, J.A., Masse, E.M., Herzberg, K.T., Meyers, M.S., Yeo, K.T., Yeo, T.K., Sioussat, T.M., and Dvorak, H.F. (1995). Pathogenesis of ascites tumor growth: vascular permeability factor, vascular hyperpermeability, and ascites fluid accumulation. Cancer Res. *55*, 360–368.

Nasarre, P., Thomas, M., Kruse, K., Helfrich, I., Wolter, V., Deppermann, C., Schadendorf, D., Thurston, G., Fiedler, U., and Augustin, H.G. (2009). Host-derived angiopoietin-2 affects early stages of tumor development and vessel maturation but is dispensable for later stages of tumor growth. Cancer Res. *69*, 1324–1333.

Nowakowski, A., Wang, C., Powers, D.B., Amersdorfer, P., Smith, T.J., Montgomery, V.A., Sheridan, R., Blake, R., Smith, L.A., and Marks, J.D. (2002). Potent neutralization of botulinum neurotoxin by recombinant oligoclonal antibody. Proc. Natl. Acad. Sci. USA *99*, 11346–11350.

Oliner, J., Min, H., Leal, J., Yu, D., Rao, S., You, E., Tang, X., Kim, H., Meyer, S., Han, S.J., et al. (2004). Suppression of angiogenesis and tumor growth by selective inhibition of angiopoietin-2. Cancer Cell *6*, 507–516.

Paez-Ribes, M., Allen, E., Hudock, J., Takeda, T., Okuyama, H., Vinals, F., Inoue, M., Bergers, G., Hanahan, D., and Casanovas, O. (2009). Antiangiogenic therapy elicits malignant progression of tumors to increased local invasion and distant metastasis. Cancer Cell *15*, 220–231.

Parikh, S.M., Mammoto, T., Schultz, A., Yuan, H.T., Christiani, D., Karumanchi, S.A., and Sukhatme, V.P. (2006). Excess circulating angiopoietin-2 may contribute to pulmonary vascular leak in sepsis in humans. PLoS Med. *3*, e46.

Saishin, Y., Takahashi, K., Lima e Silva, R., Hylton, D., Rudge, J.S., Wiegand, S.J., and Campochiaro, P.A. (2003). VEGF-TRAP(R1R2) suppresses choroidal neovascularization and VEGF-induced breakdown of the blood-retinal barrier. J. Cell. Physiol. *195*, 241–248.

Shibuya, M., and Claesson-Welsh, L. (2006). Signal transduction by VEGF receptors in regulation of angiogenesis and lymphangiogenesis. Exp. Cell Res. *312*, 549–560.

Shim, W.S., Ho, I.A., and Wong, P.E. (2007). Angiopoietin: a TIE(d) balance in tumor angiogenesis. Mol. Cancer Res. *5*, 655–665.

Tam, B.Y., Wei, K., Rudge, J.S., Hoffman, J., Holash, J., Park, S.K., Yuan, J., Hefner, C., Chartier, C., Lee, J.S., et al. (2006). VEGF modulates erythropoiesis through regulation of adult hepatic erythropoietin synthesis. Nat. Med. *12*, 793–800.

Verheul, H.M., and Pinedo, H.M. (2007). Possible molecular mechanisms involved in the toxicity of angiogenesis inhibition. Nat. Rev. Cancer *7*, 475–485.

Verheul, H.M., Hammers, H., van Erp, K., Wei, Y., Sanni, T., Salumbides, B., Qian, D.Z., Yancopoulos, G.D., and Pili, R. (2007). Vascular endothelial growth factor trap blocks tumor growth, metastasis formation, and vascular leakage in an orthotopic murine renal cell cancer model. Clin. Cancer Res. *13*, 4201–4208.

Wu, C., Ying, H., Grinnell, C., Bryant, S., Miller, R., Clabbers, A., Bose, S., McCarthy, D., Zhu, R.R., Santora, L., et al. (2007). Simultaneous targeting of multiple disease mediators by a dual-variable-domain immunoglobulin. Nat. Biotechnol. *25*, 1290–1297.

Yoshiji, H., Kuriyama, S., Noguchi, R., Yoshii, J., Ikenaka, Y., Yanase, K., Namisaki, T., Kitade, M., Uemura, M., Masaki, T., and Fukui, H. (2005). Angiopoietin 2 displays a vascular endothelial growth factor dependent synergistic effect in hepatocellular carcinoma development in mice. Gut *54*, 1768–1775.

Zhang, L., Yang, N., Park, J.W., Katsaros, D., Fracchioli, S., Cao, G., O'Brien-Jenkins, A., Randall, T.C., Rubin, S.C., and Coukos, G. (2003). Tumor-derived vascular endothelial growth factor up-regulates angiopoietin-2 in host endothelium and destabilizes host vasculature, supporting angiogenesis in ovarian cancer. Cancer Res. *63*, 3403–3412.